International Journal of
INTELLIGENT SYSTEMS AND APPLICATIONS IN ENGINEERING
ISSN:2147-6799 www.ijisae.org Original Research Paper

Homotopy Analysis Method (HAM) for an Analysis of Unsteady MHD Thin Film Nanofluid Flow over a Moving Flat Surface

Padmini [1], Jagadish V. Tawade[2*], Chandrakant Guled[3], Jayashri Sanamani [4]

Submitted: 06/05/2024 **Revised**: 19/06/2024 **Accepted**: 26/06/2024

Abstract: The flow and heat transfer properties of a nanofluid in a thin layer over stretched heat have keen applications in several contemporary processes. Indisputably, the thin film's heat transfer rate affects how the coating process is presented as well as the chemical makeup of the final result. The research presented in this article is based on the "Homotopy analysis method," a series solution for an unsteady magnetohydrodynamic thin film's unstable boundary value issue. When there is an uneven heat source or sink present, there is a nanofluid flow over the flat surface. The Homotopy research speeds up the process of ensuring that any strong nonlinearity problem's series solution will converge.

Owing to wide variety of industrial applications, we have investigated impacts of factors such as magnetic field, temperature- and space-dependent (A^*) and (B^*) across a stretched sheet in current study with flow property and displayed same visually. Furthermore, it was shown that increasing heat source/sink's non-uniform parameter decreased local Nusselt number while increasing the thermal boundary layer's thickness. The study shows that temperature field, velocity field, Nusselt number, and thin film thickness are all significantly impacted by magnetic field, thermal conductivity, and non-uniform heat source/sink characteristic. Additionally, it is evident that a rise in magnetic field parameter results in an increase in temperature profile, whereas wall friction, fluid's velocity field, and pace at which heat transfer occurs have the opposite impact.

Keywords: *Stretching surface, Non-uniform heat source/sink, Magnetohydrodynamics, Nanofluid, Homotopy analysis method.*

1. Introduction

several uses in a variety of technological domains, such as heat exchangers and solid surface coatings, food stuff striating, elastic sheet drawing, device fluidization, and polymer and metal extraction processes, has piqued the interest of researchers in studying nanofluidflow problems in recent times. . Wang [1, 2] conducted an analytical study to ascertain hydro dynamical essence of a flux's thin liquid film over a unstable stretching sheet.

For further information on the issue, see Andersson et al. [3, 4]. Further research on liquid film is considered crucial, considering its wide variety of industrial uses. As a consequence, a number of scholars [5, 6] have sometimes created important geometry constructions.In addition, a number of authors [7-22] have taken into consideration the fundamental issue raised by Wang [1, 2] and of the same Anderson et al [3, 4]. Furthermore, various intriguing occurrences are acknowledged.

Heat transfer within nanofluids has drawn attention recently from researchers in preparation for a range of industrial uses. Numerous methods exist for enhancing base fluid characteristics. For this reason, nanofluid is more advantageous in fuel cells, hybrid powered engines, microelectronic chip cooling, and many medicinal applications. According to Choi et al. [23,24], a 1% increase in nanoparticle volume yields a nearly twofold increase in thermal conductivity properties. Thin layer nanofluid heat transfer phenomena were also shown by the writers [25–31].

For a variety of non-Newtonian fluids, authors have recently examined flow across horizontal sheets. Referencing homotopy analytic technique (HAM) (Refs. [40-42]), researchers [32–39] have shown a keen interest in convergence of thin film flow issues. The boundary value problem solutions produced by HAM are superior than the current findings.

The objective of the present study is to analyse an analytical investigation for electrically conducting flow and heat transfer of a nanofluid fluid over a flat stretched surface with non-uniform heat source/sink in two-dimensional models. Because of their practical significance and extensive industrial use, the graphical and analytical results of the skin friction and Nusselt

[1]*VTURC, Department of Mathematics, Bheemanna Khandre Institute of Technology, Bhalki, INDIA*
pskaji123@gmail.com
[2]*Department of Mathematics, Vishwakarma University, Pune-411048, INDIA jagadish.tawade@vupune.ac.in*
[3]Department of Applied Sciences, Indian Institute of Information Technology Pune-411048,
Maharashtra, *INDIA*
chandrakantguled@iiitp.ac.in
[4]Science Department, Government Polytechnic Kalagi, Dist: Kalaburgi – 585101, *INDIA*
1983jayashree@gmail.com
[*] **Corresponding Author:** *jagadish.tawade@vupune.ac.in* **(Jagadish V. Tawade)**

number are also assessed. In present studies for initial estimates, consistency, quick convergence, dependability, and correctness in outcomes, the homotopy analysis approach is used and discussed with help of graphics. The contributions of recently discovered physical factors are investigated, including skin friction, magnetic field, Nusselt number, and non-uniform sink/heat source. Findings indicate that thermal boundary layer thickness has increased in heat production and absorption, which is significant for heat management operations.

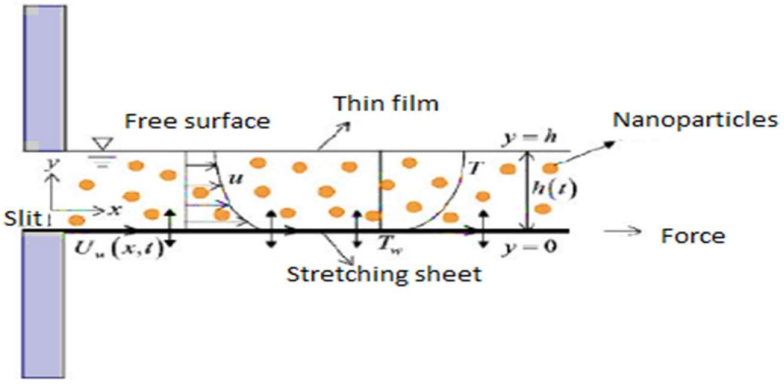

Schematic diagram of the flow problem

2. PROBLEM FORMULATION

In unstable 2-D flow, the continuity, momentum, and energy equations (Ref.fig.1) are

$$\frac{\partial u}{\partial x}+\frac{\partial v}{\partial y}=0 \dots\dots\dots\dots\dots\dots (1)$$

$$\frac{\partial u}{\partial t}+u\frac{\partial u}{\partial x}+v\frac{\partial u}{\partial y}=\frac{\mu_{nf}}{\rho_{nf}}\frac{\partial^2 u}{\partial y^2}-\sigma\frac{B^2u}{\rho} \dots\dots\dots (2)$$

$$\frac{\partial T}{\partial t}+u\frac{\partial T}{\partial x}+v\frac{\partial T}{\partial y}=\alpha_{nf}\frac{\partial^2 T}{\partial y^2}+\frac{q'''}{\rho C_p} \dots\dots\dots (3)$$

Where

$$q'''=\frac{ku_w(x)}{xv}[A^*(T_S-T_0)f'+(T-T_0)B^*] \dots (4)$$

Heat generated internally is shown by A* and B* > 0, whereas heat absorbed internally is indicated by A* and B* < 0. Using the symbols u and v, respectively, denote velocity components that are parallel and perpendicular$ to the horizontal axis. Noting that there is no liquid movement for t≤0 is necessary at this point.

In order to solve equations (1) through (3), the required conditions are Equations (1) through (3) may be solved with the following initial and boundary conditions: **2.1. Initial and boundary conditions**

$$u=0,v=0,T=T_w fort\le 0 \dots (5)$$

For $t>0$ and $x\ge 0$, boundary conditions are as below:

$$u=U,v=0,T=T_w aty=0 \dots\dots\dots (6)$$

$$\frac{\partial u}{\partial y}=\frac{\partial T}{\partial y}=0,\frac{\partial h}{\partial t}=vaty=h \dots\dots\dots (7)$$

Here, we must observe that the heat flow and viscous shear stress vanish at the adiabatic plane.

2.2. Formulation

The relevant similarity transformations that we will present are as follows:$\psi(x,y,t)=$

$$\left(\frac{v_f b}{1-\alpha t}\right)^{\frac{1}{2}} xf(\eta) \dots\dots (8)$$

$$T(x,y,t)=T_0-T_{ref}\left[\frac{bx^2}{2v_f}\right](1-\alpha t)^{-\frac{1}{2}}\theta(\eta) \dots (9)$$

$$\eta=\left[\frac{b}{v_f(1-\alpha t)}\right]^{\frac{1}{2}} y \dots\dots\dots\dots (10)$$

In this instance, u and v, the velocity components of ψ(x,y,t) are defined as

$$u=\frac{\partial\psi}{\partial y}=\left(\frac{bx}{1-\alpha t}\right)f'(\eta) \dots\dots\dots (11)$$

$$v=-\frac{\partial\psi}{\partial x}=-\left(\frac{v_f b}{1-\alpha t}\right)^{\frac{1}{2}} f(\eta) \dots\dots\dots (12)$$

In this case, the derivative is with. respect to η, and thickness of the dimensionless film, denoted by γ, is derived by using equation (10).

$$\gamma=h(1-\alpha t)^{-\frac{1}{2}}\left(\frac{b}{v_f}\right)^{\frac{1}{2}}, \dots\dots (13)$$

whichis given by

$$\frac{dh}{dt}=-(1-\alpha t)^{-\frac{1}{2}}\left(\frac{v_f}{b}\right)^{\frac{1}{2}}\frac{\alpha\gamma}{2} \dots\dots (14)$$

From governing equations (2)–(3), the following differential equations, which are of an ordinary type, may be constructed with the assistance of similarity transformation (see equations (8) to (10)).

$$f''' + \varphi_1\gamma\left(ff'' - \frac{S}{2}\eta f'' - (f')^2 - (S+M)f'\right) = 0 \quad \dots\dots\dots\dots\dots\dots\dots (15)$$

$$\theta'' + \varphi_2\left(\frac{k_f}{k_{nf}}\right)\gamma\, Pr\, Pr\, \left\{\left(f\theta' - \frac{S}{2}\eta\theta'\right) + (A^* f' + B^*\theta)\right\} = 0 \dots\dots (16)$$

Subject to boundary conditions

$$f(0) = 0, f'(0) = \theta(0) = 1 \dots\dots\dots\dots\dots\dots (17)$$

$$f''(\gamma) = \theta'(\gamma) = 0 \quad \dots\dots\dots\dots\dots\dots\dots (18)$$

$$f(\gamma) = \frac{S\gamma}{2} \dots\dots\dots\dots\dots\dots\dots\dots\dots\dots\dots\dots (19)$$

Here, γ represents the film thickness, $Pr = k_f/\left(\mu C_p\right)_{nf}$stands for Prandtl number, and S=α/b for an unsteadiness parameter on base fluid. The volume fractions $\phi_1 and\ \phi_2$are defined as follows:

$$\varphi_1 = (1-\varphi)^{\frac{5}{2}}\left[(1-\varphi) + \varphi\left(\frac{\rho_s}{\rho_f}\right)\right],$$

$$\varphi_2 = (1-\varphi)\varphi\left\{\frac{\left(\rho C_p\right)_s}{\left(\rho C_p\right)_f}\right\}$$

Heat transfer rate was defined by the Nusselt number Nu_x whereas surface drag was characterized by the skin friction coefficients C_f. The following are the formulae for τ_w, or shear stress, and forq_w, or surface heat flux.

$$\tau_w = -\mu_{nf}\left[\frac{\partial u}{\partial y}\right]_{y=0}, \qquad q_w = -k_{nf}\left[\frac{\partial T}{\partial y}\right]_{y=0}$$

$$C_f = \frac{\tau_w}{\frac{1}{2}\rho U^2} = \frac{2}{(1-\varphi)^{\frac{5}{2}}} Re^{-1/2}\{-f''(0)\} \dots (20)$$

$$Nu_x = \frac{x q_w}{k_f(T_w - T_0)} = \left(\frac{k_f}{k_{nf}}\right) Re^{-1/2}\{-\theta'(0)\} \quad (21)$$

3. HOMOTOPY ANALYSIS METHOD(HAM) SOLUTION

In order to obtain homotopy analysis solution of equations (15) to (16) with necessary boundary conditions (Ref. (17)-(19)), we go with initial guess approximations as

$$f_0(\eta) = 1 - e^{-\eta} \dots\dots\dots (22)$$

$$\theta_0(\eta) = e^{-\eta} \dots (23)$$

and the auxiliary linear operators as

$$L_f = \frac{\partial^3}{\partial\eta^3} - \frac{\partial}{\partial\eta} \dots (24)$$

$$L_\theta = \frac{\partial^2}{\partial\eta^2} - 1 \dots (25)$$

The above linear operators satisfy

$$L_f[C_1 + e^{\eta}C_2 + e^{-\eta}C_3] = 0 \dots (26)$$

$$L_\theta[e^{\eta}C_4 + e^{-\eta}C_5] = 0 \dots . (27)$$

HereC_i is an arbitrary constant (for$i = 1, 2, \dots, 5$).

Zeroth order deformation equations are constructed by selecting q as the embedding parameter, as shown below.

$$(1-q)L_f\left[\widehat{f}\,(\eta,q) - f_0(\eta)\right] = q\,\hbar_f N_f\left[\widehat{f}\,(\eta,q)\right] \quad \dots\dots\dots\dots\dots\dots\dots\dots\dots\dots (28)$$

$$(1-q)L_\theta\left[\widehat{\theta}\,(\eta,q) - \theta_0(\eta)\right] = q\,\hbar_\theta N_\theta\left[\widehat{\theta}\,(\eta,q)\right] \quad \dots\dots\dots\dots\dots (29)$$

With boundary condition

$$\widehat{f}\,(0,q) = 0, \widehat{f}\,'(0,q) = 1, \widehat{f}\,'(\infty,q) = 0 \quad \dots\dots\dots\dots (30)$$

$$\widehat{\theta}\,(0,q) = 1, \widehat{\theta}\,'(\infty,q) = 0 \quad \dots\dots (31)$$

In the above equations, prime stands for the partial derivatives with respect to η, and$\hbar_f$and $\hbar_\theta$stand for the non-zero auxiliary factors.It is also said that the nonlinear differential operators $N_f$and N_θ are

$$N_f\left[\widehat{f}\,(\eta,q)\right] = \frac{\partial^3\widehat{f}\,(\eta,q)}{\partial\eta^3} + \phi_1\gamma\left[\widehat{f}\,(\eta,q)\frac{\partial^2\widehat{f}\,(\eta,q)}{\partial\eta^2} - \frac{S\eta}{2}\frac{\partial^2\widehat{f}\,(\eta,q)}{\partial\eta^2} - \left(\frac{\partial\widehat{f}\,(\eta,q)}{\partial\eta}\right)^2 - (S+M)\frac{\partial\widehat{f}\,(\eta,q)}{\partial\eta}\right] \dots\dots\dots\dots (32)$$

$$N_\theta\left[\widehat{f}\,(\eta,q)\right] = \frac{\partial^2\widehat{\theta}\,(\eta,q)}{\partial\eta^2} + \phi_2\frac{k_f}{k_{nf}}\gamma\, Pr\left[\left\{\widehat{f}\,(\eta,q)\frac{\partial\widehat{\theta}\,(\eta,q)}{\partial\eta} - \frac{S\eta}{2}\frac{\partial\widehat{\theta}\,(\eta,q)}{\partial\eta}\right\} + \left\{A^*\frac{\partial\widehat{f}\,(\eta,q)}{\partial\eta} + B^*\theta\right\}\right] \quad (33)$$

Clearly, we have for $q = 0$and $q = 1$

$$\widehat{f}\,(\eta,0) = f_0(\eta), \qquad \widehat{f}\,'(\eta,1) = f(\eta) \dots (34)$$

$$\widehat{\theta}\,(\eta,0) = \theta_0(\eta), \ \widehat{\theta}\,'(\eta,1) = \theta(\eta) \dots (35)$$

using Taylor's series, and equations (34) & (35), we have

$$\widehat{f}\,(\eta,q) = f_0(\eta) + \sum_{m=1}^{\infty} f_m(\eta)q^m \dots (36)$$

$$\widehat{\theta}(\eta, q) = \theta_0(\eta) + \sum_{m=1}^{\infty} \theta_m(\eta) q^m \ldots . (37)$$

and

$$f_m(\eta) = \frac{1}{m!} \frac{\partial^m \widehat{f}(\eta, q)}{\partial \eta^m}|_{q=0} \ldots (38)$$

$$\theta_m(\eta) = \frac{1}{m!} \frac{\partial^m \widehat{\theta}(\eta, q)}{\partial \eta^m}|_{q=0} \ldots (39)$$

Both $\hbar_f$ and $\hbar_\theta$ are thought to be properly chosen so that equations (36) and (37) both converge at q=1. Then, because of equations (34) & (35),, we get

$$f(\eta) = f_0(\eta) + \sum_{m=1}^{\infty} f_m(\eta) \quad (40)$$

$$\theta(\eta) = \theta_0(\eta) + \sum_{m=1}^{\infty} \theta_m(\eta) \ldots . . (41)$$

and respectively.

m-th order deformation equation is generated by taking derivative of deformation equations (28) and (29) that are in the zeroth order m-times with respect to q. Derivative is then divided by the factorial of m to establish the value for q=0.

$$L_f[f_m(\eta) - \chi_m f_{m-1}(\eta)] = \hbar_f R_{m,f}(\eta) . . (42)$$

$$L_\theta[\theta_m(\eta) - \chi_m \theta_{m-1}(\eta)] = \hbar_\theta R_{m,\theta}(\eta) \ldots (43)$$

With the chosen BCs are

$$f_m(0) = f_m'(0) = f_m'(\infty) = 0 \ldots (44)$$

$$\theta_m(0) = \theta_m(\infty) = 0 \ldots (45)$$

Where $\chi_m = \{0\ , m \leq 1\ 1\ , m > 1 \ldots (46)$

and

$$R_{m,f}(\eta) = f_{m-1}''' - \phi_1 \gamma \frac{S\eta}{2} f_{m-1}'' - \phi_1 \gamma (S + M) f_{m-1}' + \phi_1 \gamma \sum_{k=0}^{m-1} [f_{m-1-k} f_k'' - f_{m-1-k}' f_k'] \ldots\ldots\ldots (47)$$

$$R_{m,\theta}(\eta) = \theta_{m-1}'' - \phi_2 \frac{k_f}{k_{nf}} \gamma\, Pr \frac{S\eta}{2} \theta_{m-1}' + \phi_2 \frac{k_f}{k_{nf}} \gamma\, Pr\, Pr\, (A^* f_{m-1}' + B^* \theta_{m-1}) + \phi_2 \frac{k_f}{k_{nf}} \gamma\, Pr \sum_{k=0}^{m-1} f_{m-1-k} \theta_k' . \ldots\ldots\ldots (48)$$

Here, to solve the eqs. (42) - (43) one after the other (for $m = 1\ ,2, 3, \ldots$), a tool MATHEMATICA is used.

4. ANALYTICAL SOLUTION SHOWING THE CONVERGENCE

As suggested by Liao [40], the auxiliary parameters $\hbar_f$ and $\hbar_\theta$play an important part in preventing the rate of approximation and convergence by HAM [41-42]. Liao [40] introduced$\hbar$ -curve that provides a tolerable range known as the convergence region, for an appropriate selection in$\hbar_f$ and $\hbar_\theta$values in order to make certain the convergences solutions in the infinite series $f(\eta)$ and $\theta(\eta)$form, respectively. In the present analysis, we have plotted $f''(0)$ versus $\hbar_f$for various values of ϕ_1 shown in figs. (13) and (14).

5. RESULTS AND DISCUSSION

Homotopy analysis method (HAM) is a analytical method which is influential mathematical tool for solving nonlinear equations. This approach enables to obtain a power series solution that may usually converge to the exact solution. In the current paper, an unsteady magnetohydrodynamic (MHD) laminar boundary layer thin film nanofluid flow has been examined analytically using HAM. Effects of temperature profile for nanofluid have been considered for volume fraction. Governing PDEs transformed into ODEs by similarity transformations. Result an t BVPs, which are nonlinear in nature (refer eqns. (15)-(19)), are solved by HAM. By solving (19), we have foundγ. Equation (15) is decoupled from (16). The two parameters S and ϕhaveaffected the flow and heat transfer within the boundary layer by keeping fixed value of Pr as 6.2 throughout the study.

It is observed that as $S \to 0$ film thickness $\gamma \to \infty$. Furthermore, as $S \to 0$, we obtain the convergent solution analytically. While$S \to 2$corresponds to an infinitesimal thickness$\gamma \to 0$. Here, a HAM solution has been achieved for $0 \leq \phi \leq 0.2\ and\ 0 \leq S \leq 2$.

Effects of magnetic field M on axial velocity profile f'(η). for various values of an unsteadiness parameter S are shown in Figs. (1)–(2). It is determined that as the magnetic field parameter values rise, fluid's velocity profile decreases.

Space-dependent effects A* on free surface temperature θ(η) are shown in Figs. (3)–(4) for S=0.8 and 1.2, respectively. Graphs show that as A*values rise, $\theta(\eta)$ increases.

Figs.(5)-(6) illustrates the effects non temperature dependent effects B^* on free surface

temperature$\theta(\eta)$ for $S = 0.8\ and\ 1.2$, respectively. The graphs reveal that the temperature profile $\theta(\eta)$ enhances with a increase in B^* values.

Figures (7)–(8) illustrate how the dimensionless free surface temperature is affected by magnetic field M for S=0.8 and 1.2, respectively. These graphs show how the fluid's surface temperature rises as the magnetic field M value of fluid increases.

It is evident from fig. (9), that as M increases, wall shear stress −f″(0) increases but wall heat flux -θ′(0) decreases (see fig. (10).

Plots (11)–(12) show that value of −θ′(0) in border area declines with increases in A* and B* for S=0.8 and 1.2, respectively.

Figures (13) through (14) show the curves of f "(0) for known values of $\phi_1$and, by utilizing 11th-order HAM approximation. Comparative findings produced by analytic solution for normal fluid (for φ = 0) are shown in Table 1. results obtained exhibit great agreement with those of Wang (2006) and Aziz et al. (2018).

Table-1: Comparison for the case of regular fluids (i.e. at Pr =1 and φ = 0)

S	Wang [2]			Aziz et al [27]			Present result		
	$-f''(0)$	$\theta(1)$	$-\theta'(1)$	$f''(0)$	$\theta(1)$	$-\theta'(1)$	$-f''(0)$	$\theta(1)$	$-\theta'(1)$
0.8	2.68094	0.097884	3.595970	2.680943	0.097956	3.591125	2.680940	0.097955	3.591130
1.0	1.97238	-	-	1.972384	0.266422	2.533515	1.972384	0.266422	2.533515
1.2	1.442631	0.286717	1.999590	1.442625	0.286717	1.999590	1.442623	0.286717	1.999590
1.4	1.012784	-	-	1.012784	0.821032	1.012784	1.012784	0.821032	1.012783
1.6	0.642397	-	-	0.642397	0.567173	1.012784	0.642397	0.567173	1.012784
1.8	0.309137	-	-	0.309137	0.356389	0.309137	0.309137	0.356389	0.309137

The $\hbar$-curve for $\theta'(0)$ is shown in the fig.(15).

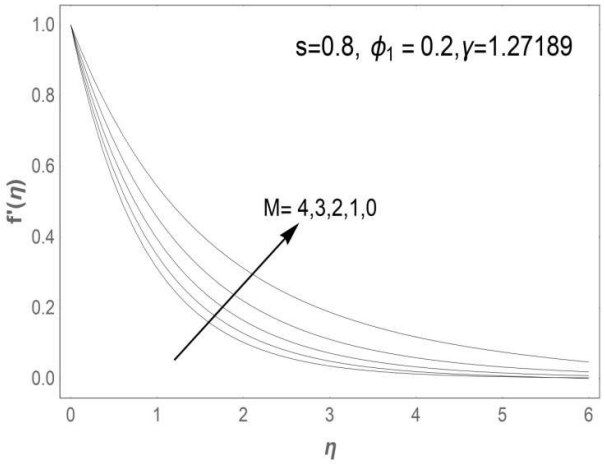

Fig.(1)

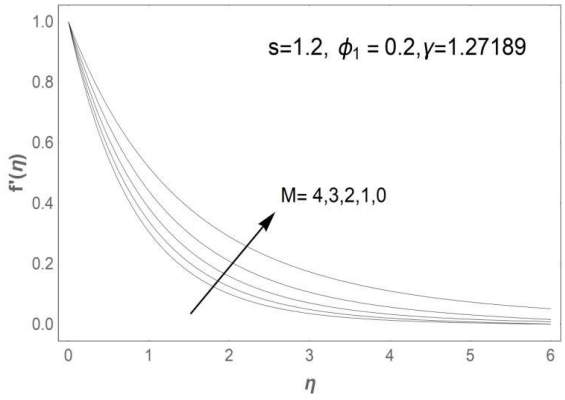

Fig.(2)

Figs. (1 & 2) represents M effects on the velocity profile $f'(\eta)$

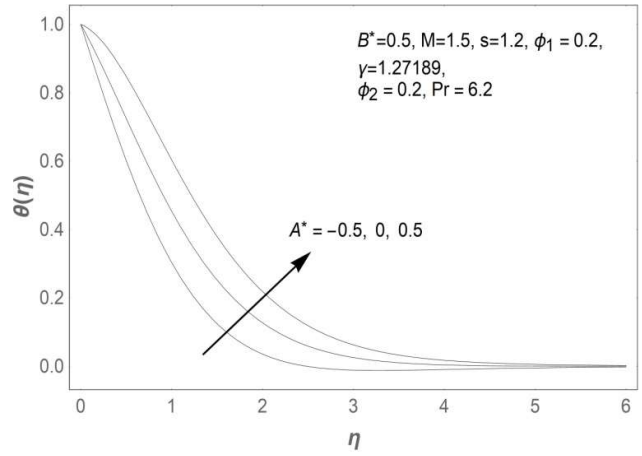

Fig.(3)

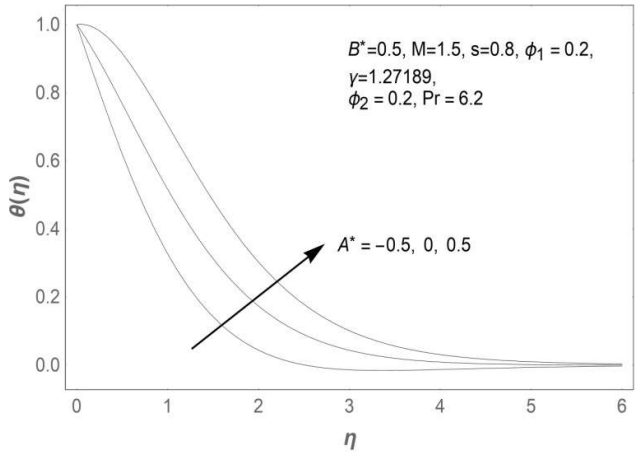

Fig.(4)

Figs. (3 & 4) represents Space-dependent A^*effects on the free surface temperature $\theta(\eta)$

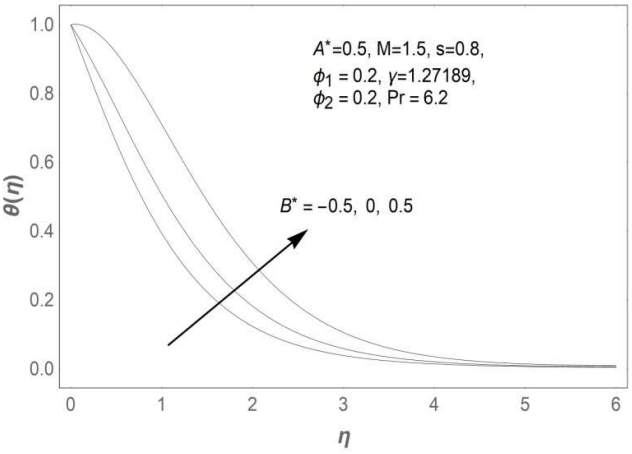

Fig.(5)

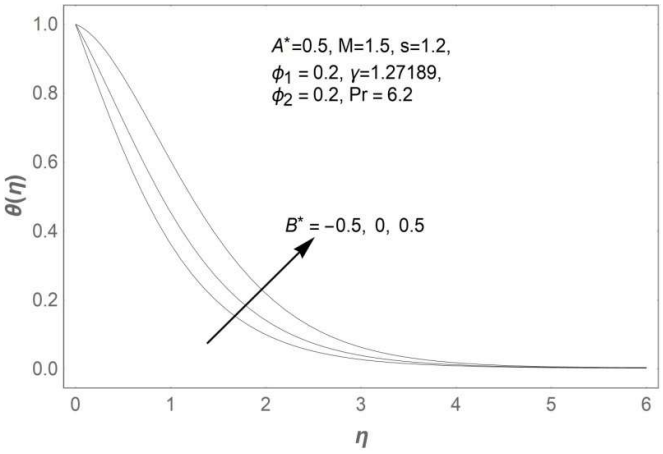

Fig.(6)

Figs. (5 & 6) represents Temperature-dependent B^*effects on free surface temperature $\theta(\eta)$

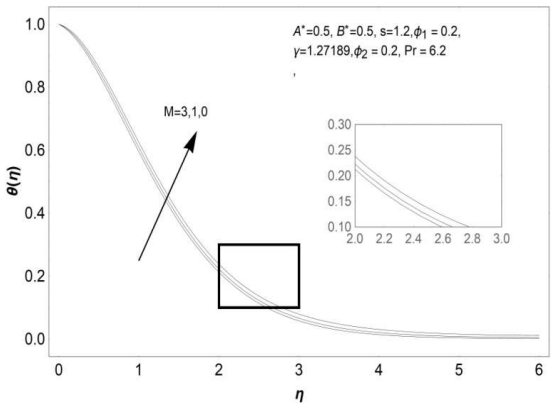

Fig.(7)

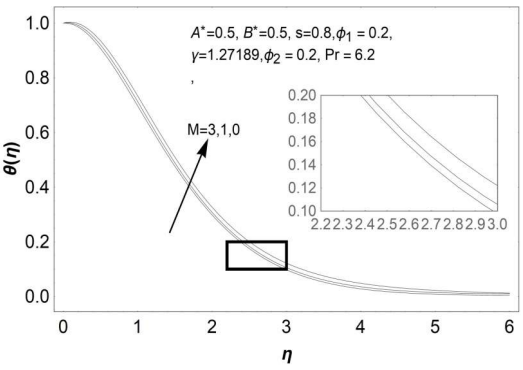

Fig.(8)

Figs. (7 & 8) represents M effects on free surface temperature $\theta(\eta)$

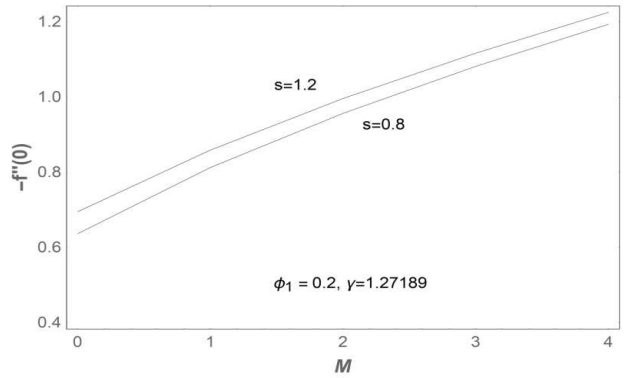

Fig.(9). Wall shear stress $-f''(0)$ $vs.$ M for special values of S

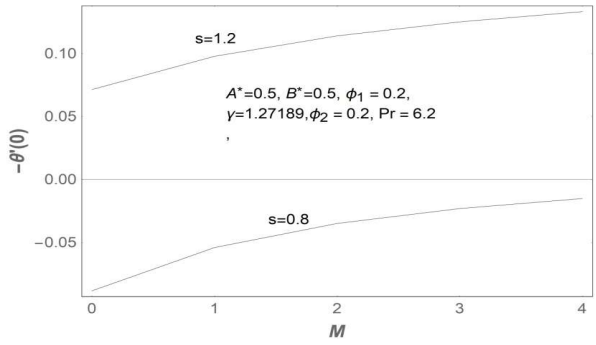

Fig.(10). Gradient of wall temperature–θ'(η) vs. M for certain values of S

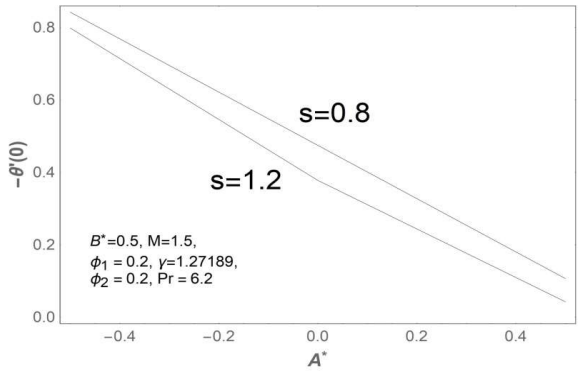

Fig.(11). Wall temperature gradient $-\theta'(0)$ $vs.$ A^* for special values of S

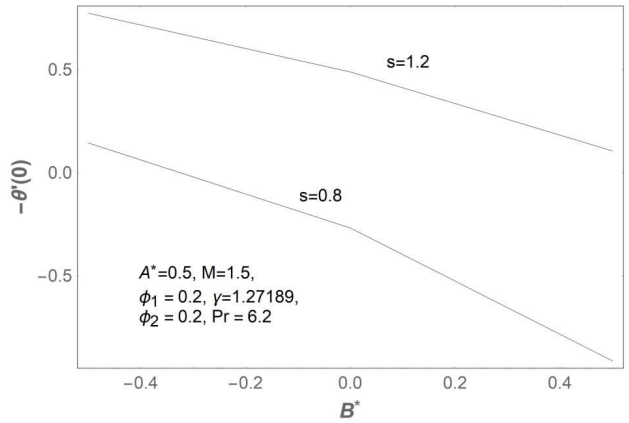

Fig.(12). Gradient of wall temperature $-\theta'(0)$ $vs.$ B^* for certain values of S

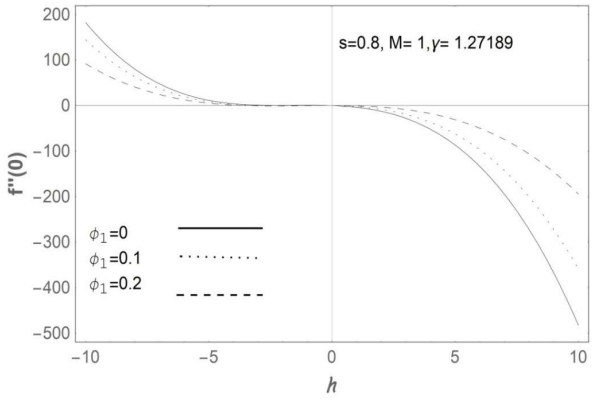

Fig. (13). $f''(0)$ curve for special values of volume fraction ϕ_1 for $S = 0.8$ using 11th-order HAM approximation

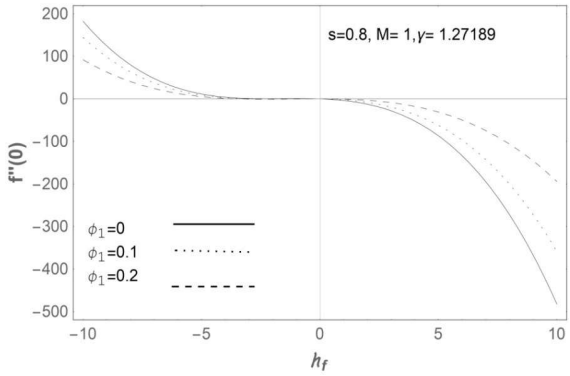

Fig.(14). $f''0)$ curve for special values of volume fraction using 11[th]-order HAM approximation

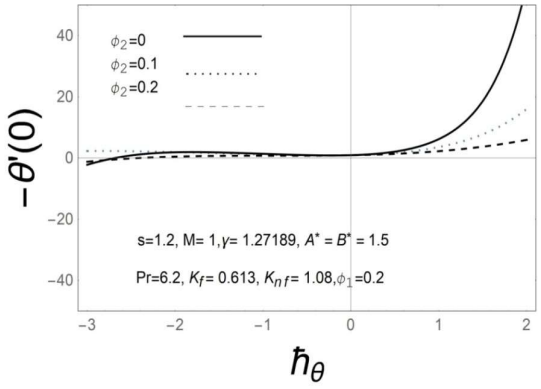

Fig.(15). $\hbar$-curve for the HAM approximation solution over $-\theta'(0)$

6. CONCLUSION

Following are key findings from HAM's current study. Dimensionless film thickness γ decreases as volume fraction parameter υ increases. Due to varying levels of S, the velocity boundary layer thickens as the nanofluid boundary layer approaches thinning.

i. An increase in ϕenhances $\theta(\eta)$thereby increases the thicknessof thermal boundary layer.

ii. $-f''(0)$, the skin friction, enriches the volume fraction ϕ

iii. $-\theta'(0)$,the dimensionlesswall temperature gradient, declines the volume fraction ϕ

iv. Thickness of thermal boundary layer enhances by heat generation/ absorption coefficients.

REFERENCES:

[1]. Wang CY. Liquid film on an unsteady stretching surface. Q Appl Math. 1990;48:601–10.

[2]. Wang C. Analytic solutions for a liquid film on an unsteady stretching surface. Heat Mass Transf. 2006;42:759–66.

[3]. Andersson HI, Aarseth JB, Dandapat BS. Heat transfer in a liquid film on an unsteady stretching surface. Int J Heat Mass Transf. 2000;43:69–74.

[4]. Liu IC, Andersson HI. Heat transfer in a liquid film on an unsteady stretching sheet. Int J Therm Sci. 2008;47:766–72.

[5]. Myers, T. Application of non-Newtonian models to thin film flow. Phys. Rev. E 2005, 72, 066302.

[6]. Marinca, V.; Heris¸anu, N.; Nemes¸, I. Optimal homotopy asymptotic method with application to thin film flow. Open Phys. 2008, 6, 648–653.

[7]. Dandapat BS, Santra B, Andersson HI. Thermocapillarity in a liquid film on an unsteady stretching surface. Int J Heat Mass Transf. 2003;46:3009–155.

[8]. Dandapat BS, Santra B, Vajravelu K. The effects of variable fluid properties and thermocapillarity on the flow of a thin film on an unsteady stretching surface. Heat Mass Transf. 2007;50:991–6.

[9]. Chen CH. Marangoni effects on forced convection of power law liquids in a thin film over a stretching surface. PhysLett A. 2007;370:51–7.

[10]. Abel MS, Mahesha N, Tawade J. Heat transfer in a liquid film over an unsteady stretching surface with viscous dissipation in presence of external magnetic field. Appl Math Model. 2009;33:3430–41.

[11]. Andersson HI, Aarseth JB, Braud N, Dandapat BS. Flow of a power-law fluid film on an unsteady stretching surface. J Nonnewton Fluid Mech. 1996;62:1–8.

[12]. Chen CH. Heat transfer in a power-law fluid film over an unsteady stretching sheet. Heat Mass Transf. 2003;39:791–6.

[13]. Chen CH. Effect of viscous dissipation on heat transfer in a non-Newtonian liquid film over an unsteady stretching sheet. J Nonnewton Fluid Mech. 2006;135:128–35.

[14]. Noor NFM, Hashim I. Thermocapillarity and magnetic field effects in a thin liquid film on an unsteady stretching surface. Int J Heat Mass Transf. 2010;53:2044–51.

[15]. Nadeem S, Awais M. Thin film flow of an unsteady shrinking sheet through porous medium with variable viscosity. PhysLett A. 2008;372:4965–72

[16]. Nadeem S, Faraz N. Thin film flow of a second grade fluid over a stretching/shrinking sheet with variable temperature-dependent viscosity. Chin PhysLett. 2010;27(3):034704.

[17]. Khan Y, Wu Q, Faraz N, Yildirim A. The effects of variable viscosity and thermal conductivity on a thin film flow over a shrinking/stretching sheet. Comput Math Appl. 2011;61:3391–9.

[18]. Khan Y, Faraz N. Thin film flow of an unsteady Maxwell fluid over a shrinking/stretching sheet with variable fluid properties. Int J Numer Meth Heat Fluid Flow. 2018;28(7):1596–612.

[19]. Kumar KA, Sandeep N, Sugunamma V, Animasaun IL. Effect of irregular heat source/sink on the radiative thin film flow of MHD hybrid ferrofluid. J Therm Anal Calorim. 2019;1:1–9.

[20]. Rehman A, Salleh Z, Gul T, Zaheer Z. The impact of viscous dissipation on the thin film unsteady flow of GO-EG/GO-W nanofluids. Mathematics. 2019;7(7):653.

[21]. Noor NFM, Abdulaziz O, Hashim I. MHD flow and heat transfer in a thin liquid film on an unsteady stretching sheet by the homotopy analysis method. Int J Numer Meth Fluids. 2010;63:357–73.

[22]. Yan Zhang, Min Zhang, Shujuan Qi, "Heat and Mass Transfer in a Thin Liquid Film over an Unsteady Stretching Surface in the Presence of Thermosolutal Capillarity and Variable Magnetic Field", Mathematical Problems in Engineering, vol. 2016, Article ID 8521580, 12 pages, 2016. https://doi.org/10.1155/2016/8521580.

[23]. Choi, S. U. S., 1995, “Enhancing Thermal Conductivity of Fluids With Nanoparticles,” Proceedings of the 1995 ASME International Mechanical Engineering Congress and Exposition, San Francisco, CA, FED231/MD66, pp. 99–105.

[24]. Choi, S. U. S., Zhang, Z. G., Yu, W., Lockwood, F. E., and Grulke, E. A., 2001, “Anomalously Thermal Conductivity Enhancement in Nanotube Suspension,” Appl. Phys. Lett., 79(14), pp. 2252–2254

[25]. Narayana M, Sibanda P. Laminar flow of a nanoliquid film over an unsteady stretching sheet. Int J Heat Mass Transf. 2012;55:7552–600.

[26]. Xu H, Pop I, You XC. Flow and heat transfer in a nano-liquid film over an unsteady stretching surface. Int J Heat Mass Transf. 2013;60:646–52.

[27]. Aziz RC, Hashim I, Abbasbandy S. Flow and heat transfer in a nanofluid thin film over an unsteady stretching sheet. SainsMalaysiana. 2018;47(7):1599–605.

[28]. Khan ZH, Qasim M, Lopez RJ. Heat and mass transfer in nanofluid thin film over an unsteady stretching sheet using buongiorno’s model. EurPhys J Plus. 2016;131(16):1–11.

[29]. Giri SS, Das K, Kundu PK. Inclined magnetic field effects on unsteady nanofluid flow and heat transfer in a finite thin film with non-uniform heat source/sink. Multidiscip Model Mater Struct. 2019;15(1):265–82.

[30]. Jawad M, Shah Z, Islam S, Khan W, Khan AZ. Nanofluid thin film flow of Sisko fluid and variable heat transfer over an unsteady stretching surface with external magnetic field. J Algorithms Comput Technol. 2018;13:1–16.

[31]. S. Maity, Y. Ghatani , B. S. Dandapat, Thermocapillary Flow of a Thin Nanoliquid Film Over an Unsteady Stretching Sheet, J. Heat Transfer. Apr 2016, 138(4): 042401 (8 pages)

[32]. Liao SJ. Proposed homotopy analysis techniques for the solution of nonlinear problems. Ph.D. Dissertation, Shanghai Jiao Tong University (1992).

[33]. Wang C, Pop I. Analysis of the flow of a power-law fluid film on an unsteady stretching surface by means

of homotopy analysis method. J Nonnewton Fluid Mech. 2006;138:161–72.

[34]. I-Chung Liu, Ahmed M. Megahed, "Homotopy Perturbation Method for Thin Film Flow and Heat Transfer over an Unsteady Stretching Sheet with Internal Heating and Variable Heat Flux", Journal of Applied Mathematics, vol. 2012, Article ID 418527, 12 pages, 2012.

[35]. I-C. Liu and A. M. Megahed , Numerical Study for the Flow and Heat Transfer in a Thin Liquid Film Over an Unsteady Stretching Sheet with Variable Fluid Properties in the Presence of Thermal Radiation, Journal of Mechanics, Volume 28, Issue 2 June 2012 , pp. 291-297.

[36]. Shah Z, Bonyah E, Islam S, Khan W, Ishaq M. Radiative MHD thin film flow of Williamson fluid over an unsteady permeable stretching sheet. Heliyon. 2018;4:e00825. doi: 10.1016/j.heliyon.2018.e00825.

[37]. Patel H.R. Effects of cross diffusion and heat generation on mixed convective MHD flow of Casson fluid through porous medium with non-linear thermal radiation. Heliyon. 2019;5

[38]. Ullah, A.; Shah, Z.; Kumam, P.; Ayaz, M.; Islam, S.; Jameel, M. Viscoelastic MHD Nanofluid Thin Film Flow over an Unsteady Vertical Stretching Sheet with Entropy Generation. Processes 2019, 7, 262.

[39]. R.C. Aziz, I. Hashim and S.Abbasbandy, Flow and Heat Transfer in a Nanofluid Thin Film over an Unsteady Stretching Sheet, SainsMalaysiana 47(7)(2018): 1599–1605

[40]. Liao SJ. Beyond perturbation: introduction to the homotopy analysis method. Boca Raton: Chapman & Hall; 2004.

[41]. Liao SJ. On the homotopy analysis method for nonlinear problems. Appl Math Comput. 2004;147:449–513.

Liao SJ. Homotopy analysis method in nonlinear differential equations. B

.